JOURNAL OF GEOPHYSICAL RESEARCH, VOL. 115, A00E40, doi:10.1029/2009JA014776, 2010

Full-wave modeling of "early" VLF perturbations caused by lightning electromagnetic pulses

Nikolai G. Lehtinen,[1] Robert A. Marshall,[1] and Umran S. Inan[1,2]

Received 14 August 2009; revised 10 December 2009; accepted 28 December 2009; published 3 July 2010.

[1] We use the three-dimensional full-wave method and Born approximation technique to calculate the scattered VLF field in the near zone of ionospheric disturbances created by lightning electromagnetic pulses. The method fully accounts for the anisotropicity of the ionosphere magnetized by a nonvertical geomagnetic field. We calculate the VLF amplitude perturbation on the ground for vertical and horizontal lightning discharge configurations. The results show that the magnitude of the scattered signal is strongly dependent on the direction of the incident VLF wave.

Citation: Lehtinen, N. G., R. A. Marshall, and U. S. Inan (2010), Full-wave modeling of "early" VLF perturbations caused by lightning electromagnetic pulses, *J. Geophys. Res.*, *115*, A00E40, doi:10.1029/2009JA014776.

1. Introduction

[2] "Early" perturbations of VLF signals [e.g., *Inan et al.*, 1995] are caused by a direct effect of lightning on the ionosphere, in contrast to the delayed perturbations caused by lightning-induced electron precipitation (LEP) from the radiation belts. In this paper we consider perturbations caused by the change in ionization caused by a lightning electromagnetic pulse (EMP) [*Taranenko et al.*, 1993; *Cheng and Cummer*, 2005; *Marshall et al.*, 2008, 2010]. The EMP also produces optical emissions named "elves" (see, e.g., review by *Rodger* [1999]). Several cases of VLF perturbations associated with elves were observed by *Mika et al.* [2006], who describes in detail a ~0.2 dB perturbation observed at a distance of 400 km from the disturbance, ~10° off the great circle path between VLF transmitter and receiver. Elve-associated VLF perturbations are usually caused by lightning discharges with typical peak currents $I > 100$ kA, and have amplitude changes usually in the range of 0.2–0.7 dB [*Mika et al.*, 2006], usually positive (i.e., increase of VLF amplitude).

[3] The scattered field in the far zone of an ionospheric disturbance, i.e., the scattering radiation diagram, has been calculated using the mode theory in Born approximation by previous workers [*Crombie*, 1964; *Wait*, 1964], who also used additional assumptions about the smoothness of the disturbance which allowed them to use the WKB approximation. Their method has been applied, for example, in the context of HF heater-induced disturbances [*Barr et al.*, 1985; *Demirkol*, 1999]. In this paper, we do not make assumptions about the smoothness of the disturbance, which allows us to calculate the full mode contents of the scattered waves.

2. Method of Calculation

2.1. Incident VLF Transmitter Wavefield

[4] The Earth-ionosphere waveguide modes and antenna excitation factors in the current work were calculated using the full-wave method [*Lehtinen and Inan*, 2008, 2009] and an approach analogous to that utilized in the LWPC model [*Pappert and Ferguson*, 1986]. All amplitudes below denote complex amplitudes of the values with time dependence $\propto e^{-i\omega t}$. We use a coordinate system with x, y in the horizontal plane and z vertical upward.

[5] Free waves (i.e., without sources) propagating in the Earth-ionosphere waveguide in the positive x-direction with horizontal refractive index $n_x = k_x/k_0$ (where $k_0 = \omega/c$ and k_x is the horizontal wave vector) are calculated from the modal equation [see also *Budden*, 1961, equation (9.28)]

$$\det\left(\mathsf{I} - \mathsf{R}^{\mathrm{d}}\mathsf{R}^{\mathrm{u}}\right) = 0 \tag{1}$$

where R^{u}, R^{d} are the 2×2 matrices representing reflection coefficients from above and from below, evaluated at the ground level using the full-wave method [*Lehtinen and Inan*, 2008] for complex n_x. The mode field structure as a function of altitude, also called the "height gain," is calculated from the eigenvector equation corresponding to (1):

$$\left(\mathsf{I} - \mathsf{R}^{\mathrm{d}}\mathsf{R}^{\mathrm{u}}\right)\mathbf{u}_0 = 0$$

where $\mathbf{u}_0$ is a column vector of length 2 which contains upward wave amplitudes at h_0. The wave amplitudes at all other altitudes and fields $\mathbf{E}(z)$, $\mathbf{H}(z)$ (e.g., the height gain) are calculated as explained by *Lehtinen and Inan* [2008]. Using this procedure, we obtain a set of modes, with pth mode characterized by height gains $\{\mathbf{E}(z), \mathbf{H}(z)\}_p$ and horizontal refactive index $(n_x)_p$. In this paper, we use the LWPC nomenclature in which the modes are labeled QTMn and QTEn, with $n \geq 1$. We decide whether the mode is QTM or

[1]Space, Telecommunications and Radioscience Laboratory, Electrical Engineering Department, Stanford University, Stanford, California, USA.
[2]Koç University, Rumelifeneri Yolu, 34450 Sariyer, Istanbul, Turkey.

0148-0227/10/2009JA014776

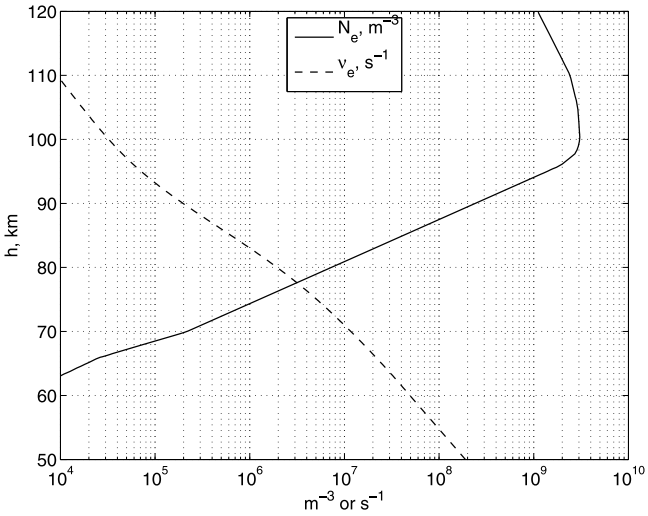

Figure 1. The used altitude profiles of ambient electron density N_e and electron-neutral collision frequency ν_e.

QTE by evaluating contributions of TM and TE components below ionosphere. The number of the mode n is calculated by ordering the modes of the same kind (QTM or QTE) in the order of increasing vacuum vertical wave number ($= k_0\sqrt{1-(n_x)_p^2}$).

[6] The mode excitation factors for a vertical ground-based electric dipole with current moment amplitude S (i.e., current density $\mathbf{J} = \hat{z}S\delta(x)\delta(y)\delta(z)$) are calculated on the basis of the theory of mode biorthogonality, explained in detail by *Pappert and Smith* [1972]. The pth mode excitation factor is

$$A_p = -SE^a_{pz}(0)$$

where $E^a_{pz}(z)$ is the E_z component of the adjoint mode $\{\mathbf{E}, \mathbf{H}\}^a_p$, which is defined in the Earth-ionosphere waveguide with the same electron density and collision frequency profiles but the reversed x-component of the geomagnetic field. The adjoint modes have the same eigenvalues $(n_x)_p$ and are biorthogonal to the original waveguide modes $\{\mathbf{E}, \mathbf{H}\}_q$, with normalization

$$\int_{-\infty}^{+\infty}\left(H^a_{pz}E_{qy} - H^a_{py}E_{qz} - E^a_{pz}H_{qy} + E^a_{py}H_{qz}\right)dz = \delta_{pq}$$

The field at $x > 0$, $y = 0$ for a medium with a vertical axis of symmetry (i.e., with vertical geomagnetic field) is given by

$$\{\mathbf{E}, \mathbf{H}\} = \sum_p A_p\{\mathbf{E}, \mathbf{H}\}_p \frac{k_0(n_x)_p}{2} H_0^{(1)}\left(k_0(n_x)_p x\right) \qquad (2)$$

where $H_0^{(1)}$ is the Hankel function representing an outward propagating cylindrical wave. In the asymmetric case, we have to take into account that the horizontal refractive index $(n_x)_p$ depends on the direction of propagation x, and therefore the group velocity for horizontal mode propagation is not parallel to the horizontal wave vector. In such a case we have to use a different $(n_{x'})_p$ which gives the group velocity along x. However, the calculations show that the dependence on the direction is rather weak: for the case considered in section 3, the relative variation $|(n_{x'})_p - (n_x)_p|/|(n_x)_p|$ in the horizontal refractive index does not exceed 0.02% for QTM1 mode and 0.2% for QTM2 mode. Therefore we may safely assume that x' and x directions are the same and use this relation. One can derive equation (2) starting with expression for the plane waves $\{\mathbf{E}, \mathbf{H}\}_{\text{line}} = \sum_p A_p\{\mathbf{E}, \mathbf{H}\}_p e^{ik_0(n_x)_p|x|}$ generated by a line dipole source $\mathbf{J}_{\text{line}} = \hat{z}S\delta(x)\delta(z)$ and representing the point source as a linear combination of line sources using technique developed, e.g., by *Budden* [1961].

[7] At the location of a disturbance, we neglect the cylindrical spreading of the VLF transmitter wave and assume it to be flat in the y-direction. This may be done when the size of the disturbance, as well as the distance from the disturbance to a receiver are both $\ll r$, the distance to the VLF transmitter. Using the asymptotic approximation of the Hankel function $H_0^{(1)}$, we have

$$\{\mathbf{E}, \mathbf{H}\} = K\sum_p \sqrt{(n_x)_p}A_p\{\mathbf{E}, \mathbf{H}\}_p e^{ik_0(n_x)_p x} \qquad (3)$$

where $K = \sqrt{k_0/(2\pi i r)}$ is a constant which takes into account the cylindrical spreading at distance r, and x is now calculated in reference to the center of the disturbance.

2.2. Born Approximation for Scattered Waves

[8] The incident wave is assumed to be one of the calculated Earth-ionosphere waveguide modes. The scattered waves may then be calculated using the full-wave method, by employing the Born approximation [*Born and Wolf*, 1999, p. 504] as outlined below.

[9] The total electric field of the VLF wave, $\mathbf{E}$, is the sum of the incoming $\mathbf{E}_0$ and scattered $\mathbf{E}_s$ fields, i.e., $\mathbf{E} = \mathbf{E}_0 + \mathbf{E}_s$. The exact wave equation for $\mathbf{E}$ is

$$\nabla \times (\nabla \times \mathbf{E}) - k_0^2\hat{\varepsilon}\mathbf{E} = 0 \qquad (4)$$

where $\hat{\varepsilon} = \hat{\varepsilon}_0 + \Delta\hat{\varepsilon}$ is the total dielectric permittivity tensor, consisting of stratified part $\hat{\varepsilon}_0$ and inhomogeneous change $\Delta\hat{\varepsilon}$. By using the unperturbed waveguide relation $\nabla \times (\nabla \times \mathbf{E}_0) - k_0^2\hat{\varepsilon}_0\mathbf{E}_0 = 0$, we can rearrange the wave equation (4) as follows:

$$\nabla \times (\nabla \times \mathbf{E}_s) - k_0^2\hat{\varepsilon}_0\mathbf{E}_s = k_0^2\Delta\hat{\varepsilon}(\mathbf{E}_0 + \mathbf{E}_s) \qquad (5)$$

The Born approximation is based on the assumption that the field inside the scattering region is $\mathbf{E}_0$, i.e., we neglect the scattered field $\mathbf{E}_s$ on the right-hand side of (5). We regard the change in the currents induced in the perturbed region as the new source of reradiated waves:

$$\nabla \times (\nabla \times \mathbf{E}_s) - k_0^2\hat{\varepsilon}_0\mathbf{E}_s \approx k_0^2\Delta\hat{\varepsilon}\mathbf{E}_0 = ik_0Z_0\Delta\mathbf{J}$$

where Z_0 is the impedance of free space and $\Delta\mathbf{J} = -ik_0\Delta\hat{\varepsilon}\mathbf{E}_0/Z_0$ are additional currents induced by the VLF wave due to the change in $\hat{\varepsilon}$. Note that if the accuracy of the Born approximation is insufficient, the second Born approximation may be applied [*Born and Wolf*, 1999, p. 708] which consists of substituting the calculated in the described manner scattered field $\mathbf{E}_s$ into the right-hand side of equation (5).

3. Results

[10] The Earth-ionosphere waveguide model used in the present work has the same ionosphere parameters as in the

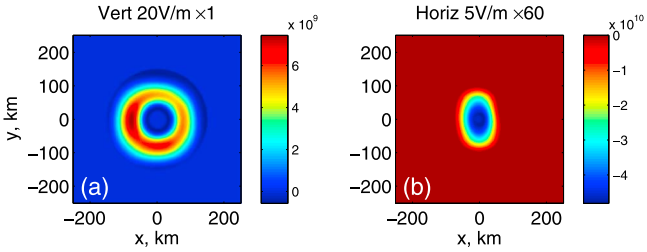

Figure 2. The top view of the change in height-integrated electron contents, in m^{-2} [*Marshall et al.*, 2010], for the two cases considered. The magnetic field is at $\phi_B = 0$, i.e., in (x, z) plane.

work of *Marshall et al.* [2010]: we use the nighttime electron density profile and the electron-neutral collision frequency from *Schunk and Nagy* [1980] (plotted in Figure 1), and the geomagnetic field $\mathbf{B}_E$ is characterized by its components in spherical coordinates, i.e., the absolute value $B_E = 5 \times 10^{-5}$ T, the polar angle $\theta_B = 45°$, and the azimuthal angle ϕ_B, which we vary in our calculations. Note that since the z component of $\mathbf{B}_E$ is positive, the present calculations correspond to the Southern Hemisphere.

[11] The mode height gains and horizontal wave numbers were calculated at a VLF frequency of $f = 24$ kHz. At this point, we apply the full-wave method by dividing the ionosphere in the range from 60 to 120 km into uniform horizontally infinite slabs of vertical thickness of 0.17 km. The modes are propagating in the positive x direction. The contributions of modes to the signal from the transmitter depend both on the excitation factors A_p and the attenuation (characterized by Im n_x) over the distance to the transmitter d, as given by equation (3). We found that, e.g., for d = 2000 km the greatest contribution (50–77% of Poynting flux on the ground, depending on ϕ_B) comes from the QTM1 mode and the second greatest contribution (17–32%) comes from QTM2. The mode height gains and wave numbers are calculated for a flat ionosphere, since the full-wave method utilized here does not yet include the Earth's curvature; the effects thereof are discussed in section 4.

[12] We consider two cases of a lightning EMP creating an initial disturbance, i.e., the change of electron density in the ionosphere which was calculated by *Marshall et al.* [2010]: (1) a single vertical discharge with $E_{100} = 20$ V/m (corresponding to peak current $I = 75$ kA) and (2) a sequence of 60 horizontal discharges at the altitude of 5 km with $E^{ic}_{100} = 5$ V/m, resulting in an accumulation of the electron density change. The measure of the discharge strength E_{100} is the electric field at 100 km distance introduced by *Orville* [1991]. The measure E^{ic}_{100} for intracloud (horizontal) discharge is the field that would be measured 100 km in the vertical direction, in the absence of an ionosphere and reflecting ground [*Marshall*, 2009, p. 85].

[13] In case 1 (vertical discharge), the relative change in the electron density is in the range from −0.1% to 1.2% and absolute change in the range from -2×10^5 m^{-3} to 3×10^6 m^{-3}, with the maximum absolute change achieved at altitude of ~90 km. In case 2 (series of 60 horizontal discharges), the relative change is in the range from −7% to 0 and absolute change in the range -10^7 m^{-3} to 0, with the maximum absolute change achieved also at altitude of ~90 km. The top view of the height-integrated change in the electron contents for both cases is shown in Figure 2. To calculate the scattered signal in the Born approximation, we again apply the full-wave method. At this point, the iono-

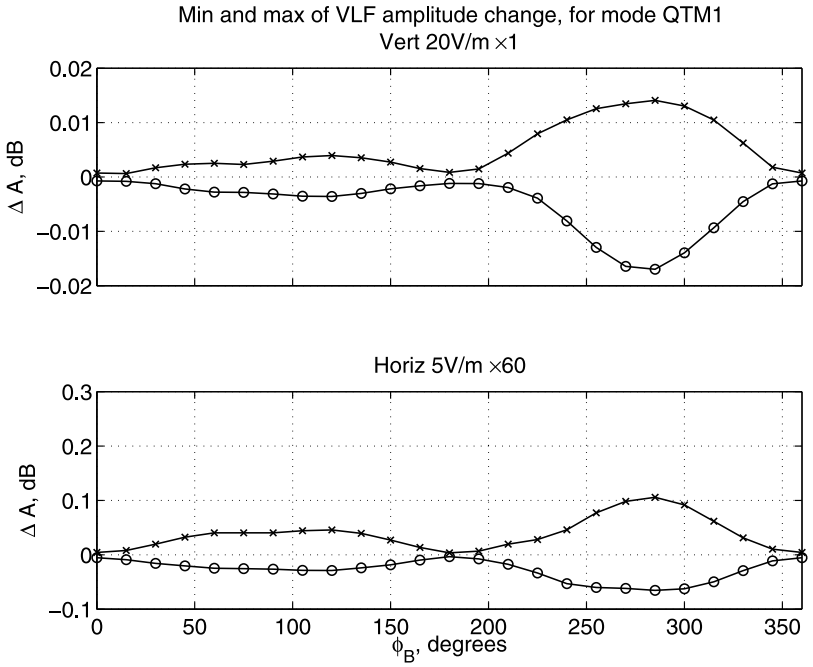

Figure 3. The maximum negative (circles) and positive (crosses) relative VLF amplitude change ΔA defined in equation (6) on the ground for different directions of the geomagnetic field, for the incident wave given by mode QTM1. The maximum is taken over the location of the receiver.

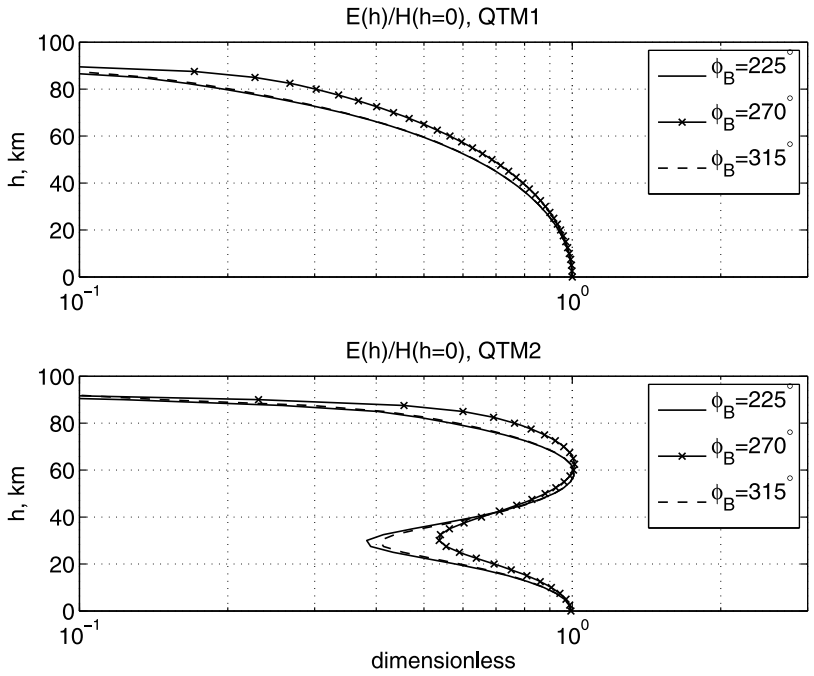

Figure 4. Height gains of QTM1 and QTM2 modes for various ϕ_B in the vicinity of ϕ_B = 270°, represented by the ratio of |**E**| to the horizontal magnetic field on the ground (H is in V/m [*Budden*, 1985, p. 31].)

sphere in the range from 60 to 120 km is divided into uniform horizontally infinite slabs of vertical thickness of 0.84 km.

[14] The electromagnetic field on the ground was calculated using the Born approximation, for the QTM1 mode with ϕ_B varying over the full circle at intervals of 15°. Since the Earth is assumed perfectly conducting, only the horizontal magnetic and vertical electric field components are nonzero. The ratio of the total magnetic field $\mathbf{B} = \mathbf{B}_0 + \mathbf{B}_s$ (where $\mathbf{B}_s$ is the scattered field) to the field in the incident wave $\mathbf{B}_0$ represents the VLF amplitude change and was calculated in dB as:

$$\Delta A = 20 \log \frac{|\mathbf{B}|}{|\mathbf{B}_0|} \tag{6}$$

The maximum and mininum amplitude change (for different directions of the geomagnetic field) are plotted in Figure 3. The maximum is taken over the location of the receiver. We see that the scattering is strongest around ϕ_B = 270°, corresponding to the incident wave propagating in the westward direction in the Southern Hemisphere.

[15] The stronger scattering in this particular direction of the geomagnetic field $\mathbf{B}_E$ can be understood when we consider the dependence of the height gain of the QTM1 mode on ϕ_B. The ionospheric disturbance caused by the lightning EMP is located in the D region, at $h \sim$ 80–90 km. In Figure 4 we observe that the electric field is relatively stronger at these altitudes at ϕ_B = 270° than at the neighboring angles. This fact is correlated with a higher absorption of the modal waves, since the absorption is mostly due to finite conductivity in the D region.

[16] The observed change in the VLF signal amplitude is strongly dependent on the position of the observer with respect to the location of the ionospheric disturbance. Figure 5 shows the 2-D structure of the amplitude change in dB on the ground, for both the vertical and horizontal discharge cases and for ϕ_B = 270°, which gives the strongest scattering. We see that the pattern is rather complicated for the vertical discharge case, because the scattering occurs on a ring-shaped disturbance (see Figure 2a). The shape of the disturbance created by the horizontal discharge case (Figure 2b) is simpler, but still the scattered field shows the near-zone pattern due to the finite size of the scattering region. The scattered wave may interfere both constructively and destructively with the incident wave, and therefore the observed change in VLF amplitude may be both positive and negative, a result also obtained with 2-D FDFD simulations by *Marshall et al.* [2008]. Figure 5 shows an absence of backscattering of the VLF wave from the disturbance, which holds true also for other values of ϕ_B. In Born approximation, the backscattering is expected to be weak from objects larger than the wavelength, such as the EMP-ionized regions of ionosphere. However, the backscattering from sprites, which may have horizontal scales comparable or smaller than the VLF wavelength, has been observed in the past [*Dowden et al.*, 1996; *Marshall et al.*, 2006].

4. Discussion

4.1. Born Approximation Validity

[17] As we discussed above, the Born approximation is valid when we can neglect the scattered field $\mathbf{E}_s$ in comparison to the incident field $\mathbf{E}_0$ in the perturbed region. To check this condition, we calculated the ratio of the two fields $|\mathbf{E}_s|/|\mathbf{E}_0|$ at the altitude of the maximum disturbance $|\Delta\mathbf{J}|$. We found that this ratio does not exceed 0.06 for the vertical discharge case and 0.2 for the horizontal discharge case.

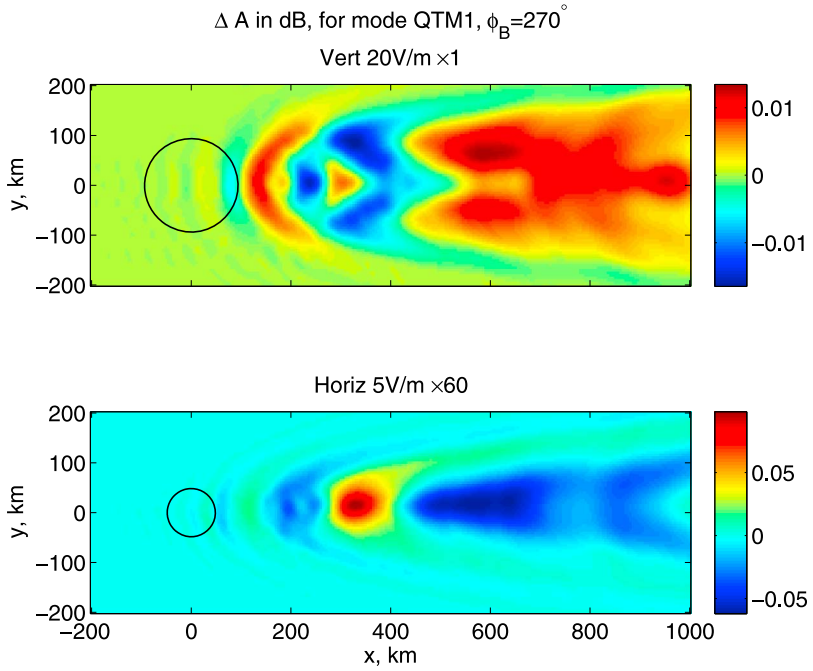

Figure 5. The VLF amplitude change ΔA on the ground as a function of the position of the receiver, for an incident QTM1 mode. The location of the disturbance is marked by a circle, and the incident wave propagates in $+x$ direction. The geomagnetic field is at ϕ_B = 270°, corresponding to the incident wave propagating in the westward direction in the Southern Hemisphere.

This number may be used as an estimate for the upper bound on the relative error in the calculated scattered field on the ground. The qualitative conclusions about the observed field therefore are not modified.

4.2. Stronger Discharges

[18] We have performed similar calculations for higher discharge values, namely vertical discharges at E_{100} = 30 V/m and 40 V/m, and horizontal discharges with 60 pulses and E^{ic}_{100} = 7 V/m and 10 V/m. For the highest values, the calculated maximum VLF amplitude reached 0.1 dB for the vertical and 5 dB for the horizontal discharge case. Discharges having higher peak currents create high changes in electron density, which constitute a large fraction of the background. Therefore the Born approximation may become invalid. However, it may be possible to use the present method by employing the second and higher Born approximations. These calculations are beyond the scope of the present paper and will to be performed in future work.

4.3. Other Modes

[19] We estimated above that at d = 2000 km distance from the transmitter the second strongest contribution to the incident VLF wave power after the QTM1 mode is made by the QTM2 mode, at the ϕ_B-dependent fraction of 17–32% in Poynting flux at the ground level. The calculations show that the scattering of the QTM2 mode is qualitatively similar to QTM1, with some quantitative differences. For example, the maximum change in VLF amplitude is higher: at ϕ_B = 270° we obtained ~0.06 dB for vertical and ~0.3 dB for horizontal discharge cases.

4.4. Observed Asymmetry in the Sign of the "Early" VLF Perturbations

[20] The scattered wave may interfere both constructively and destructively with the incident wave, and therefore the observed change in the VLF amplitude may be both positive and negative, which was also confirmed by the 2-D FDFD simulations of *Marshall et al.* [2008]. The same authors also proposed that in some cases, electron depletion caused by dissociative attachment to molecular oxygen should lead to lower absorption and therefore a positive average VLF perturbation. For a horizontal disturbance size d the maximum improvement is $\exp[k_0(\mathrm{Im}\, n_x)\, d]$. For the QTM1 mode and d = 100 km this is <0.035 dB and for QTM2, <0.25 dB, while the experimentally observed asymmetry is still present at >1 dB [*Marshall et al.*, 2008, Figure 3]. From this estimate it follows that to agree with experimental statistics, the average disturbance has to have a large (>400 km) size.

[21] If the incident wave is very weak, due, e.g., to the destructive interference between waveguide modes, then the scattered wave may greatly exceed the incident wave and there should be more positive perturbations. For the asymmetry due to this effect to manifest itself, the ratio of scattered to incident amplitudes has to be at least a factor of two, which corresponds to ~6 dB. However, the experimental asymmetry [*Marshall et al.*, 2008, Figure 3] is very pronounced at the lower range of 0.5–1.5 dB.

[22] We have performed a statistical analysis of the calculated VLF amplitude perturbations, which is presented in Figure 6. We show the distribution of ΔA in dB for a randomly positioned receiver, for the QTM1 mode for both the vertical and horizontal discharge cases. The amplitude of the scattered wave is falling to zero as the receiver is being

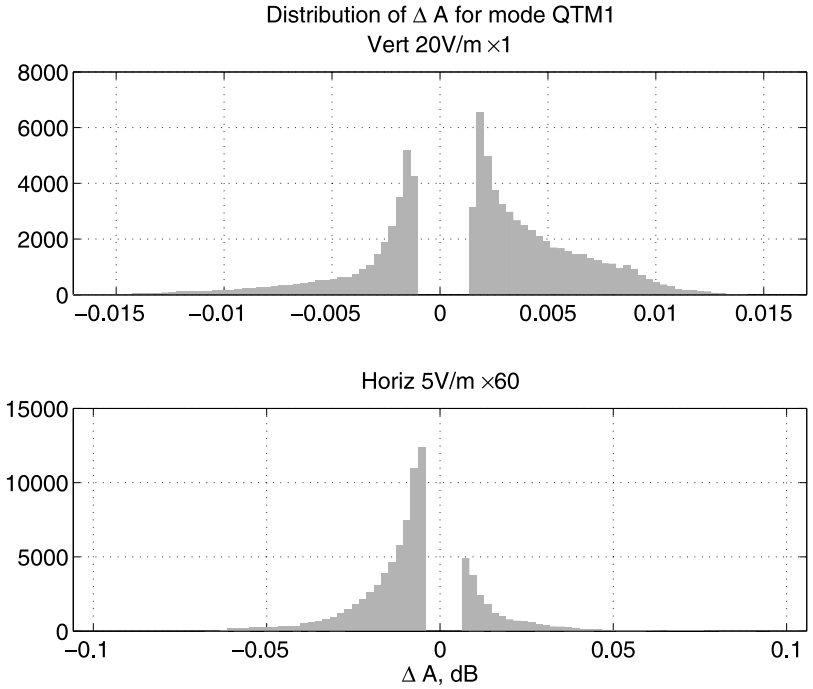

Figure 6. Distribution of VLF amplitude changes ΔA in dB, for the QTM1 mode for both the vertical and horizontal discharge cases. The receiver position is random and uniformly distributed in a rectangular horizontal area of 1200 × 400 km around the disturbance (such as depicted in Figure 5). Also, the azimuthal angle ϕ_B of the geomagnetic field is random and uniformly distributed in (0, 2π). The small VLF amplitude changes (less than the typical values on the edges of the above mentioned horizontal area) are excluded from the statistics.

moved to greater distances from the scattering region, and at the same time the position of the receiver may be randomly chosen over a greater area. Thus the small VLF perturbations are more likely to be seen then the large ones. Since the calculation results are available only for small distances (inside the rectangle shown in Figure 5), for the purpose of the statistical analysis in Figure 6 we limit ourselves only to the higher-amplitude perturbations. Namely, the VLF perturbations with values less than the typical values on the edges of the region being modeled were removed from the histograms in Figure 6.

[23] In Figure 6 one may observe that our calculations produce a small asymmetry in the VLF amplitude perturbations. There seem to be more positive perturbations for the vertical discharge and more negative perturbations for the horizontal discharge. This may be related to the different shapes of the ionospheric disturbances produced by these two types of discharges. However, we currently do not understand the mechanism that would explain this asymmetry. Note that the asymmetry is in the opposite sense as would be expected from the hypothesis by *Marshall et al.* [2008], taking into account the sign of electron density change in Figure 2. Analogous calculations taken separately for mode QTM2 give the same qualitative result, i.e., there seem to be more positive perturbations for the vertical discharge and more negative perturbations for the horizontal discharge.

4.5. Direction of the Geomagnetic Field

[24] The calculations are performed with a positive vertical component of $\mathbf{B}_E$, same as in the work of *Marshall et al.* [2010], which corresponds to the geomagnetic field in the Southern Hemisphere. However, many observations [e.g., *Mika et al.*, 2006] were performed in the Northern Hemisphere. To understand how the calculations would change in the Northern Hemisphere, we may use the symmetry transformation, in which all spatial coordinates and vectors undergo an inversion (i.e., we take a mirror image), and in addition the magnetic field vector changes its polarity. Thus the calculated maximum scattering at $\phi_B = 270°$ corresponds to incident waves traveling in the westward direction in both Southern and Northern Hemispheres.

4.6. Earth Curvature Effects

[25] The distances between the ionospheric disturbance and the receiver considered in this work are much smaller than the radius of the Earth. However, the finite curvature of the Earth surface is expected to be manifested as modifications of the height gains of the waveguide modes. In the curved coordinates, the analog of Snell's law is $\mathbf{n}_\perp r = const$ [*Budden*, 1985, p. 564]. From this law it follows that in a uniform medium, the height gain decreases with altitude faster than in flat geometry. This can be understood if we consider the vertical component n_z, which is increasing with altitude. Since n_z is small for the QTM1 and QTM2 modes (which propagate almost horizontally), the mode wave experiences a total internal reflection as it propagates downward from high altitudes. At the caustic surface of the total internal reflection (corresponding approximately to the surface of the Earth), the amplitude of the wave is large. Thus the ratio plotted in Figure 4 is expected to be smaller at

the altitude of the ionospheric disturbance [see also *Poulsen*, 1992, p. 41], and therefore should lead to a smaller scattered field. However, this claim has to be verified by a rigorous calculation in curved geometry.

5. Summary

[26] We have calculated the near-zone field of the VLF waves scattered by ionospheric disturbances. The basic results of this work are the following: (1) The scattered field creates a complicated 2-D pattern on the ground which will produce both positive and negative VLF perturbations, depending on the position of the receiver. (2) The VLF perturbations are maximal for westward propagating VLF modes, for ionospheric disturbances occurring in both Southern and Northern Hemispheres. (3) The backscattered wave amplitude is below observable values. (4) There seem to be more positive perturbations for the vertical discharge and more negative perturbations for the horizontal discharge, although the mechanism of this asymmetry is not clear.

[27] **Acknowledgments.** This work was supported by the High-Frequency Active Auroral Research Program (HAARP), the Air Force Research Laboratory (AFRL), the Defense Advanced Research Program Agency (DARPA), and the Office of Naval Research (ONR) via ONR grant N00014-05-1-0854 and by NSF/CEDAR grant ATM-0535461 to Stanford University. We are grateful to Timothy F. Bell for many useful discussions of mode theory.

[28] Amitava Bhattacharjee thanks the reviewers for their assistance in evaluating this paper.

References

Barr, R., M. T. Rietveld, P. Stubbe, and H. Kopka (1985), The diffraction of VLF radio waves by a patch of ionosphere illuminated by a powerful HF transmitter, *J. Geophys. Res.*, *90*(A3), 2861–2875, doi:1029/JA090iA03p02861.

Born, M., and E. Wolf (1999), *Principles of Optics: Electromagnetic Theory of Propagation, Interference and Diffraction of Light*, 7th ed., Cambridge Univ. Press, Cambridge, U. K.

Budden, K. G. (1961), *The Wave-Guide Mode Theory of Wave Propagation*, Prentice-Hall, Englewood Cliffs, N. J.

Budden, K. G. (1985), *The Propagation of Radio Waves: The Theory of Radio Waves of Low Power in the Ionosphere and Magnetosphere*, Cambridge Univ. Press, Cambridge, U. K.

Cheng, Z., and S. A. Cummer (2005), Broadband VLF measurements of lightning-induced ionospheric perturbations, *Geophys. Res. Lett.*, *32*, L08804, doi:10.1029/2004GL022187.

Crombie, D. D. (1964), The effects of a small local change in phase velocity on the propagation of a VLF radio signal, *J. Res. Natl. Bur. Stand. U.S., Sect. D*, *68*, 709–715.

Demirkol, M. K. (1999), VLF remote sensing of the ambient and modified lower ionosphere, Ph.D. thesis, Stanford Univ., Stanford, Calif.

Dowden, R. L., J. B. Brundell, W. A. Lyons, and T. E. Nelson (1996), Detection and location of red sprites by VLF scattering of subionospheric transmissions, *Geophys. Res. Lett.*, *23*(14), 1737–1740, doi:10.1029/96GL01697.

Inan, U. S., T. F. Bell, V. P. Pasko, D. D. Sentman, E. M. Wescott, and W. A. Lyons (1995), VLF signatures of ionospheric disturbances associated with sprites, *Geophys. Res. Lett.*, *22*(24), 3461–3464, doi:10.1029/95GL03507.

Lehtinen, N. G., and U. S. Inan (2008), Radiation of ELF/VLF waves by harmonically varying currents into a stratified ionosphere with application to radiation by a modulated electrojet, *J. Geophys. Res.*, *113*, A06301, doi:10.1029/2007JA012911.

Lehtinen, N. G., and U. S. Inan (2009), Full-wave modeling of transionospheric propagation of VLF waves, *Geophys. Res. Lett.*, *36*, L03104, doi:10.1029/2008GL036535.

Marshall, R. A. (2009), Very low frequency radio signatures of transient luminous events above thunderstorms, Ph.D. thesis, Stanford Univ., Stanford, Calif.

Marshall, R. A., U. S. Inan, and W. A. Lyons (2006), On the association of early/fast very low frequency perturbations with sprites and rare examples of VLF backscatter, *J. Geophys. Res.*, *111*, D19108, doi:10.1029/2006JD007219.

Marshall, R. A., U. S. Inan, and T. W. Chevalier (2008), Early VLF perturbations caused by lightning EMP-driven dissociative attachment, *Geophys. Res. Lett.*, *35*, L21807, doi:10.1029/2008GL035358.

Marshall, R. A., U. S. Inan, and V. S. Glukhov (2010), Elves and associated electron density changes due to cloud-to-ground and in-cloud lightning discharges, *J. Geophys. Res.*, *115*, A00E17, doi:10.1029/2009JA014469.

Mika, Á., C. Haldoupis, T. Neubert, R. R. Su, H. T. Hsu, R. J. Steiner, and R. A. Marshall (2006), Early VLF perturbations observed in association with elves, *Ann. Geophys.*, *24*, 2179–2189.

Orville, R. E. (1991), Calibration of a magnetic direction finding network using measured triggered lightning return stroke peak currents, *J. Geophys. Res.*, *96*(D9), 17,135–17,142, doi:10.1029/91JD00611.

Pappert, R. A., and J. A. Ferguson (1986), VLF/LF mode conversion model calculations for air to air transmissions in the earth-ionosphere waveguide, *Radio Sci.*, *21*(4), 551–558, doi:10.1029/RS021i004p00551.

Pappert, R. A., and R. R. Smith (1972), Orthogonality of VLF height gains in the earth ionosphere waveguide, *Radio Sci.*, *7*(2), 275–278, doi:10.1029/RS007i002p00275.

Poulsen, W. L. (1992), Modeling of very low frequency wave propagation and scattering within the Earth-ionosphere waveguide in the presence of lower ionospheric disturbances, Ph.D. thesis, Stanford Univ., Stanford, Calif.

Rodger, C. J. (1999), Red sprites, upward lightning, and VLF perturbations, *Rev. Geophys.*, *37*(3), 317–336, doi:10.1029/1999RG900006.

Schunk, R. W., and A. F. Nagy (1980), Ionospheres of the terrestrial planets, *Rev. Geophys.*, *18*(4), 813–852, doi:10.1029/RG018i004p00813.

Taranenko, Y. N., U. S. Inan, and T. F. Bell (1993), Interaction with the lower ionosphere of electromagnetic pulses from lightning: heating, attachment, and ionization, *Geophys. Res. Lett.*, *20*(15), 1539–1542, doi:10.1029/93GL01696.

Wait, J. R. (1964), On phase changes in very-low-frequency propagation induced by an ionospheric depression of finite extent, *J. Geophys. Res.*, *69*(3), 441–445, doi:10.1029/JZ069i003p00441.

U. S. Inan, N. G. Lehtinen, and R. A. Marshall, STAR Laboratory, Stanford University, 350 Serra Mall, Stanford, CA 94305, USA. (nleht@stanford.edu)